Evidence for inverse-Compton emission from globular clusters

Song, D.; Macias, O.; Horiuchi, S.; Crocker, R.M.; Nataf, D.M.

Evidence for inverse-Compton emission from globular clusters

Deheng Song,[a,*] **Oscar Macias,**[a,b,c] **Shunsaku Horiuchi,**[a] **Roland M. Crocker**[d] **and David M. Nataf**[e]

[a]*Center for Neutrino Physics, Department of Physics, Virginia Tech, Blacksburg, VA 24061, USA*

[b]*Kavli Institute for the Physics and Mathematics of the Universe (WPI),University of Tokyo, Kashiwa, Chiba 277-8583, Japan*

[c]*GRAPPA Institute, Institute of Physics, University of Amsterdam, 1098 XH Amsterdam, The Netherlands*

[d]*Research School of Astronomy and Astrophysics, Australian National University, Canberra, ACT 2611, Australia*

[e]*Center for Astrophysical Sciences and Department of Physics and Astronomy, The Johns Hopkins University, Baltimore, MD 21218, USA*

E-mail: dhsong@vt.edu

Millisecond pulsars are very likely the main source of gamma-ray emission from globular clusters. However, the relative contributions of two separate emission processes–curvature radiation from millisecond pulsar magnetospheres vs. inverse Compton emission from relativistic pairs launched into the globular cluster environment by millisecond pulsars–have long been unclear. To address this, we search for evidence of inverse Compton emission in 8-year *Fermi*-LAT data from the directions of 157 Milky Way globular clusters. We find that the γ-ray luminosities of the globular clusters are correlated with their stellar encounter rates (6.4σ) and total radiation field energy density (3.8σ). We demonstrate that the gamma-ray emission of globular clusters can be resolved spectrally into two components: i) an exponentially cut-off power law and ii) a pure power law. The latter component–which we uncover at a significance of 8.2σ–is most naturally interpreted as inverse Compton emission by cosmic-ray electrons and positrons injected by millisecond pulsars. The luminosity of this inverse Compton component suggests that the fraction of millisecond pulsar spin-down luminosity into relativistic leptons is similar to the fraction of the spin-down luminosity into prompt magnetospheric radiation.

*Presenter

1. Introduction

Over two dozen globular clusters (GCs) have been detected in γ rays in *Fermi* Large Area Telescope (LAT) data and the millisecond pulsar (MSP) populations of those GCs are most likely the main source of this γ-ray emission. Here, motivated by the increasing number of GCs detected in γ rays, we perform a collective statistical study of their properties to gain insight into the nature of their high-energy emission. Our particular aim is to investigate the importance of the contribution of inverse Compton (IC) emission to the overall γ-ray emission (including the curvature radiation [CR] from the pulsar magnetosphere) of GCs.

Relations between the detected GC gamma-ray luminosities and properties of GC can be used to probe the origins of γ-ray emission and their underlying sources. For example, correlations with the photon field energy density of GCs could unveil the potential contribution from IC, and correlations with the stellar encounter rate and metallicity could provide insight into the dynamical formation of MPSs in GCs.

In parallel, modeling of GCs' observed broadband spectral energy distributions provides a handle on their CR and IC emissions. Recently, Ref. [1] and Ref. [2] modelled the multiwavelength emission from MSPs considering a potential CR origin for GeV and IC emissions for TeV γ rays, as well as synchrotron radiation for the radio and X-ray wavebands. These models are successful in explaining the multiwavelength spectra of Terzan 5. However, Terzan 5 is the only GC (perhaps) detected above TeV energies [3]. Detailed spectral modelling similar to that presented in Ref. [1] and Ref. [2] is difficult for other GCs at present due to a lack of TeV γ-ray data.

In the recently published *Fermi*-LAT fourth source catalog [4] (4FGL), 30 GCs have been detected in GeV γ rays. With such a number, we can begin to carefully study the nature of the γ-ray emission from GCs through a population study. Here, we repeat the bin-by-bin analysis of the 4FGL data for the 157 known Milky Way GCs in the Harris catalog (2010 edition) [5]. We search for correlations between the γ-ray luminosity of the GCs and other parameters of the GCs to probe which are good proxies for the γ-ray luminosity and study the potential IC contributions; to this end, we consider the photon field energy densities, the stellar encounter rate, and the metallicity of the GCs. Unlike previous studies of correlations of the GC γ-ray emissions, we consider also the upper limits placed by null detections, which we implement via a Kendall τ coefficient test statistic. Furthermore, we also look for evidence of IC from the spectra of GCs. For the first time, we implement a universal two-component model to study the spectra of γ-ray-detected GCs. The two-component model comprises a CR component, which is spectrally curved, plus an IC component modeled as a power law in the energy range of interest.

2. Gamma-ray emission from globular clusters

Here, we reanalyse the publicly available *Fermi*-LAT data from the direction of all GCs in the Harris catalog, which contains identifications and basic parameters for 157 GCs in the Milky Way.

The origin of the γ-ray emission from GCs can be studied by comparing its dependency on GC properties. For example, IC emission may be sensitive to the ambient photon field on which the $e^{\pm}$ scatter [6]. We extract the energy density of the interstellar radiation at the locations of the GCs from the three-dimensional interstellar radiation model in `GALPROP v56` [7, 8]. In addition,

photons from stars in the GCs are expected to make a dominant contribution to the total ambient radiation field. We estimate this component by

$$u_{GC} = \frac{L_*}{4\pi c r_h^2},$$

(1)

where L_* and r_h are the stellar luminosity and the half-light radius of the GC. The total photon field energy density is $u_{Total} = u_{MW} + u_{GC}$. A potential correlation between the γ-ray luminosity L_γ and the stellar encounter rate has been studied as a way to probe the dynamic formation of MSPs in GCs [6, 9, 10]. We adopt the stellar encounter rate estimated by [11]. Additionally, it has been argued [6, 10] that high metallicity [Fe/H] in the GCs could enhance the dynamical formation of MSP. We use the GCs metallicities reported in the [5] catalog, which summarizes spectroscopic or photometric estimates in the literature. In summary, we consider the empirical dependence of the inferred γ-ray luminosity of GCs on four parameters, namely, u_{MW}, u_{Total}, Γ_c, and [Fe/H].

We use 8 years of *Fermi*-LAT data, from 2008 August 4 to 2016 August 2. This constitutes the same data as the 4FGL. The newest Pass 8 data release is applied. The event class for the analysis is "P8 Source" class (evclass=128) and the event type is "FRONT+BACK" (evtype=3). We use a 90° zenith angle cut to remove Earth limb events and filter the data by (DATA_QUAL>0)&&(LAT_CONFIG==1). The corresponding instrument response function is P8R3_SOURCE_V2.

For 30 GCs detected by the 4FGL, we simply reanalyse the 4FGL γ-ray source. We use a 10° by 10° Region-of-Interest around the source with a 0.1° by 0.1° bin size. Photons from 300 MeV to 500 GeV are analysed using 9 logarithmic bins. The most recent Galactic interstellar emission model gll_iem_v07 and the isotropic component iso_P8R3_SOURCE_V2_v1 are employed as fore/backgrounds with free-floating normalization. The spectral parameters of the 4FGL sources lying within 5° of the Region-of-Interest center are allowed to float freely.

For the 127 additional GCs in the Harris catalog without 4FGL detection, we estimate the 95% C.L. γ-ray upper limits from their locations. More specifically, we place a point source at the coordinates of those GCs. The point source is assumed to have a power-law spectrum $dN/dE \sim E^{-\Gamma}$ with fixed index $\Gamma = 2$. We applied the same pipeline used on the set of detected GCs and obtained the 95% C.L. flux upper limits on the putative point sources placed at the GCs locations.

3. Correlation analysis

To study the correlations between the L_γ's and the other GC observables, we assume a linear relation in logarithmic space of the form:

$$\log(L_\gamma) = a \log(X) + b,$$

(2)

where L_γ is the gamma-ray luminosity of the GC, X is the independent observable considered, and a and b are parameters to be determined.

We use an expectation-maximization (EM) algorithm [12–14] to find the maximum likelihood estimates of the parameters a and b. In contrast to the standard maximum likelihood method, the EM algorithm is designed to be used with censored data, i.e., data consisting of both measurements and limits. Upper limits must be properly incorporated in the correlation analyses to obtain statistically

Table 1: Summary of correlations between L_γ and two astrophysical parameters of the GCs. The best-fit parameters a, b are found using the EM algorithm. The significance of the correlations is found by MC simulations with Kendall τ coefficients.

Correlation	a	b	Significance
vs Γ_c	0.39 ± 0.10	32.99 ± 0.26	6.4σ
vs u_{Total}	0.59 ± 0.09	32.97 ± 0.19	3.8σ
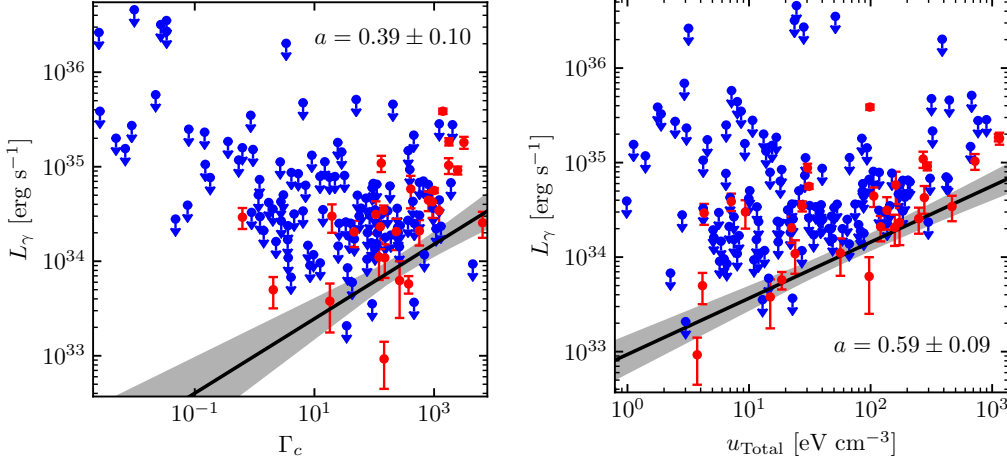
Figure 1: Correlations with the L_γ. The left panel shows the L_γ-Γ_c correlation and the right panel shows the L_γ-u_{Total} correlation. GCs with measured γ rays are shown in red, while GCs with upper limits are shown in blue. The best-fit correlations (black solid lines) are calculated using the EM algorithm, with 1σ uncertainties included as the gray shaded bands.

robust results. Using the EM algorithm, we are able to utilize the complete data set (including upper limits) in estimating the relations between the L_γ and the other observables.

We are also interested in determining the statistical significance of the relations. To that end, we apply the generalized Kendall τ rank correlation test and perform Monte Carlo (MC) simulations following a similar procedure as advanced previously in the literature for multiwavelength correlations of star-forming galaxies [15, 16], and misaligned active galactic nuclei [17].

Using the tools described above, we find two correlations that are statistically significant. They are the correlations of L_γ-u_{Total} and L_γ-Γ_c. The left panel of Figure 1 shows the correlations between L_γ and Γ_c. GCs with measured γ-ray luminosity are shown in red, while GCs with upper limits are shown in blue. We find a positive correlation between the L_γ and Γ_c, with $a = 0.39 \pm 0.10$, for which the Kendall τ test yields a 6.4σ statistical significance. In the right panel of Figure 1, we find a L_γ-u_{Total} correlation with $a = 0.59 \pm 0.09$. In this case, the significance is 3.8σ. No significant correlations are found between L_γ and other parameters. We summarize the best-fit correlation results and their respective statistical significance in Table 1.

The positive L_γ-u_{Total} correlation could indicate a significant contribution from IC emission. If the $e^\pm$ injected by MSPs lose energy through multiple comparable processes, e.g., IC and synchrotron radiaton, the L_γ is proportional to the IC energy loss rates, which is linearly proportional

to the u_{Total}. In the extreme limit where all the $e^{\pm}$ injected by MSPs lose their energy through IC, the L_{γ} is constrained by the energy injection rate of $e^{\pm}$ by MSPs and the u_{Total} would have less impact. Since we find a preference for a non-linear correlation ($a = 0.59 \pm 0.09$), the γ rays are unlikely all originated from IC radiation. In the meanwhile, the positive correlation between L_{γ} and u_{Total} could alternatively be driven by the L_{γ}–Γ_c correlation since the data of u_{Total} and Γ_c can be also correlated. Therefore, the correlation found between L_{γ} and u_{Total} is indicative but cannot be considered as concrete evidence for IC. However, evidence for IC emission in GCs may still be revealed from the detailed spectral properties of these objects.

4. Spectral analysis

We perform a spectral analysis of the 30 GCs detected in the 4FGL catalog, with the aim of finding further evidence for IC emission. We fit, bin-by-bin, the GCs' spectra using a linear combination of the CR and IC spectral components:

$$\frac{dN}{dE} = \left[\frac{dN}{dE}\right]_{\text{CR}} + \left[\frac{dN}{dE}\right]_{\text{IC}} = N_1 \left(\frac{E}{E_0}\right)^{-\Gamma_1} \exp\left(-\frac{E}{E_{\text{cut}}}\right) + N_2 \left(\frac{E}{E_0}\right)^{-\Gamma_2}. \tag{3}$$

Fitting such a two-component model to each GC's bin-by-bin data is difficult since the GC spectra only contains 9 energy bins, and many high energy bins only provide upper limits. On the other hand, typical GCs can host close to ~ 20 MSPs [18] each. So, as a simplifying approximation, we hypothesise that the γ-ray and $e^{\pm}$ injection from the collection of MSPs in each GC to be similar to one another. Then, we can fit a universal spectral shape to all γ-ray detected GCs, i.e., one set of spectral shape parameters in the two-component model in equation (3) for all the GCs. More specifically, we tie the Γ_1, Γ_2 and E_{cut} across all GCs considered. The normalization factors N_1 and N_2 are allowed to float for each GC as these should depend on the number of MSPs and the photon field energy density in the GCs.

We perform the universal fit by minimizing the total χ^2 of 30 γ-ray-detected GCs,

$$\chi^2_{\text{total}}(\Gamma_1, \Gamma_2, E_{\text{cut}}) = \sum_i \chi^2_i(\Gamma_1, \Gamma_2, E_{\text{cut}}, N_1^i, N_2^i). \tag{4}$$

By scanning the parameter space of Γ_1, Γ_2, and E_{cut}, we find the values that minimize the total χ^2 for the two-component model. These are,

$$\Gamma_1 = 0.88 \pm 0.44,$$

$$\Gamma_2 = 2.79 \pm 0.25,$$

$$\log\left(\frac{E_{\text{cut}}}{\text{MeV}}\right) = 3.28 \pm 0.16,$$

for which we find a $\chi^2_{\text{total}}/\text{d.o.f} = 204/206 = 0.99$.

The corresponding null hypothesis to the universal model contains only the CR component. Again, we tie Γ_1 and E_{cut} across all GCs and allow the normalization factors to individually vary. We find that the best-fit parameters for the CR-only model are:

$$\Gamma_1 = 1.72 \pm 0.21,$$

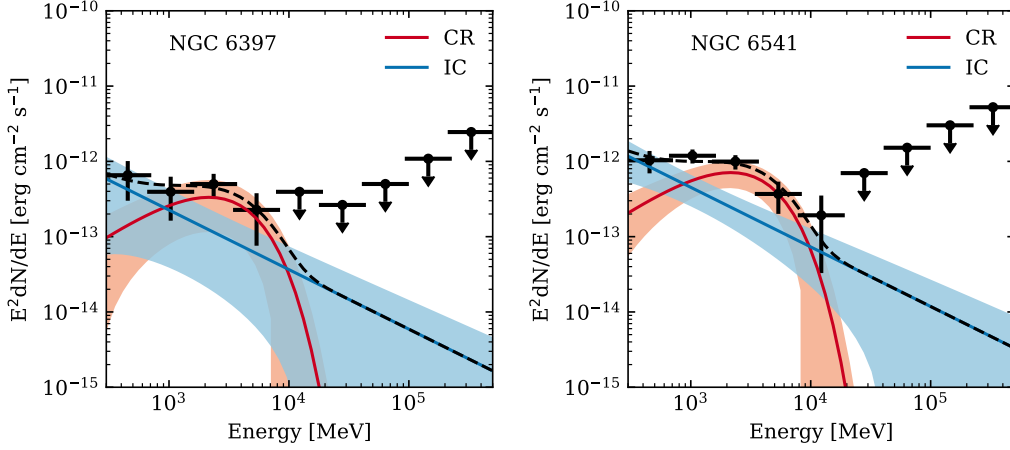$$\log\left(\frac{E_{\text{cut}}}{\text{MeV}}\right) = 3.53 \pm 0.19.$$

Figure 2: The best-fit two-component spectra for NGC 6397 (left) and NGC 6541 (right). The spectra are fit to a universal shape with same Γ_1, Γ_2, and E_{cut} for all GCs. Only the normalizations of the two components are allowed to vary between GCs. The best-fit parameters for the CR component (red line with shaded band) is $\Gamma_1 = 0.88 \pm 0.44$ and $\log(E_{\text{cut}}/\text{MeV}) = 3.28 \pm 0.16$. The best fit parameter for the IC component (blue line with shaded band) is $\Gamma_2 = 2.79 \pm 0.25$. The black dashed line indicates the total of the two components.

In this case, we find a $\chi^2_{\text{total}}/\text{d.o.f} = 349/237 = 1.47$. This implies that the two-component model is preferred at the 8.2σ level.

We show examples of the spectra obtained in the universal fit of the two-component model for NGC 6397 and NGC 6541 in Figure 2. As can be seen, the solutions for the CR and IC components look physically plausible. The spectra also include 1σ bow-tie errors, which immediately reveal the level of statistical support for the CR and IC components, respectively.

For 19 GCs (out of the 30 GCs included in the universal fit), we find good statistical support for both the CR and IC models. For the remaining 11 GCs, we find that only one component is sufficient to explain the spectrum: 7 GCs require only the CR model and the other 4 GCs require only the IC model.

To explain the best-fit power law index of the IC component ($\Gamma_2 = 2.79 \pm 0.25$), the implied emitting $e^\pm$ spectrum would have an index of 4.58 ± 0.50. The minimum $e^\pm$ energy required to maintain a power law IC in the energy range of our analysis (300 MeV) is $\lesssim 10$ GeV given that the upscattered photon field has energies ~ 1 eV [19]. Interestingly, [20] has simulated $e^\pm$ pair cascades from pulsar polar caps. For typical MSP parameters, they show that the injected $e^\pm$ flux decreases by $\sim 5 - 10$ orders of magnitude when the $e^\pm$ energy increases from ~ 10 GeV to ~ 1 TeV. The soft $e^\pm$ spectrum we found is in line with their results.

The relative normalization of the CR and IC components probes an important property of the MSPs: the γ-ray production and $e^\pm$ injection efficiencies, respectively. Indeed, the spin-down energy of MSPs can be injected into γ rays and $e^\pm$. While prompt γ rays are mainly produced by CR in the magnetosphere, the $e^\pm$ can propagate into the interstellar environment and lose energy. In the approximation that IC is the leading energy loss process, we can estimate the ratios between the γ-ray efficiency f_γ and the $e^\pm$ efficiency $f_{e^\pm}$ of the MSPs for different GCs using the luminosity

of the CR and IC components found in the spectral analysis,

$$\frac{f_{e^\pm}}{f_\gamma} \simeq \frac{L_{\text{IC}}}{L_{\text{CR}}}. \tag{5}$$

These are found to be in the range $\approx 0.17 - 1.04$. The measurement of pulsars by *Fermi*-LAT estimated the f_γ efficiency from observations of pulsars and found that on average, $f_\gamma \sim 10\%$ [21].

5. Conclusions

We have reanalyzed *Fermi*-LAT data from the direction of 157 Milky Way globular clusters. We have found that the gamma-ray luminosity of globular clusters are correlated with their steller encounter rates and total raditaion field. Our analysis has also revealed strong evidence for a soft inverse Compton component in the energy spectra of *Fermi*-LAT globular clusters. Based on the discovery, the $e^\pm$ efficiency of the millisecond pulsars hosted by the globular clusters is estimated to be comparable to, or slightly smaller than their γ-ray efficiency, which is about 10%. Forthcoming TeV telescopes such as CTA [22] and LHAASO [23] may detect such an inverse Comtpon signal from the globular clusters [24] or Galactic center region [25, 26].

Acknowledgements

References

[1] A. Kopp, C. Venter, I. Büsching, and O. C. de Jager, ApJ **779**, 126 (2013).

[2] H. Ndiyavala, C. Venter, T. J. Johnson, A. K. Harding, D. A. Smith, P. Eger, A. Kopp, and D. J. van der Walt, ApJ **880**, 53 (2019), 1905.10229.

[3] H. E. S. S. Collaboration, A. Abramowski, F. Acero, F. Aharonian, A. G. Akhperjanian, G. Anton, A. Balzer, A. Barnacka, U. Barres de Almeida, Y. Becherini, et al., A&A **531**, L18 (2011), 1106.4069.

[4] S. Abdollahi, F. Acero, M. Ackermann, M. Ajello, W. B. Atwood, M. Axelsson, L. Baldini, J. Ballet, G. Barbiellini, D. Bastieri, et al., ApJS **247**, 33 (2020), 1902.10045.

[5] W. E. Harris, AJ **112**, 1487 (1996).

[6] C. Y. Hui, K. S. Cheng, Y. Wang, P. H. T. Tam, A. K. H. Kong, D. O. Chernyshov, and V. A. Dogiel, ApJ **726**, 100 (2011), 1101.4107.

[7] T. A. Porter, G. Jóhannesson, and I. V. Moskalenko, ApJ **846**, 67 (2017), 1708.00816.

[8] G. Jóhannesson, T. A. Porter, and I. V. Moskalenko, ApJ **856**, 45 (2018), 1802.08646.

[9] A. A. Abdo, M. Ackermann, M. Ajello, L. Baldini, J. Ballet, G. Barbiellini, D. Bastieri, R. Bellazzini, R. D. Blandford, E. D. Bloom, et al., A&A **524**, A75 (2010), 1003.3588.

[10] R. de Menezes, F. Cafardo, and R. Nemmen, MNRAS **486**, 851 (2019), 1811.06957.

[11] A. Bahramian, C. O. Heinke, G. R. Sivakoff, and J. C. Gladstone, ApJ **766**, 136 (2013), 1302.2549.

[12] E. D. Feigelson and P. I. Nelson, ApJ **293**, 192 (1985).

[13] T. Isobe, E. D. Feigelson, and P. I. Nelson, ApJ **306**, 490 (1986).

[14] M. P. Lavalley, T. Isobe, and E. D. Feigelson, in *Bulletin of the American Astronomical Society* (1992), vol. 24, pp. 839–840.

[15] M. Ackermann, M. Ajello, A. Allafort, L. Baldini, J. Ballet, D. Bastieri, K. Bechtol, R. Bellazzini, B. Berenji, E. D. Bloom, et al., ApJ **755**, 164 (2012), 1206.1346.

[16] M. Ajello, M. Di Mauro, V. S. Paliya, and S. Garrappa, ApJ **894**, 88 (2020), 2003.05493.

[17] M. Di Mauro, F. Calore, F. Donato, M. Ajello, and L. Latronico, ApJ **780**, 161 (2014), 1304.0908.

[18] C. S. Ye, K. Kremer, S. Chatterjee, C. L. Rodriguez, and F. A. Rasio, ApJ **877**, 122 (2019), 1902.05963.

[19] G. R. Blumenthal and R. J. Gould, Reviews of Modern Physics **42**, 237 (1970).

[20] A. K. Harding and A. G. Muslimov, ApJ **743**, 181 (2011), 1111.1668.

[21] A. A. Abdo, M. Ajello, A. Allafort, L. Baldini, J. Ballet, G. Barbiellini, M. G. Baring, D. Bastieri, A. Belfiore, R. Bellazzini, et al., ApJS **208**, 17 (2013), 1305.4385.

[22] Cherenkov Telescope Array Consortium, B. S. Acharya, I. Agudo, I. Al Samarai, R. Alfaro, J. Alfaro, C. Alispach, R. Alves Batista, J. P. Amans, E. Amato, et al., *Science with the Cherenkov Telescope Array* (2019).

[23] X. Bai, B. Y. Bi, X. J. Bi, Z. Cao, S. Z. Chen, Y. Chen, A. Chiavassa, X. H. Cui, Z. G. Dai, D. della Volpe, et al., arXiv e-prints arXiv:1905.02773 (2019), 1905.02773.

[24] H. Ndiyavala, P. P. Krüger, and C. Venter, MNRAS **473**, 897 (2018), 1708.09817.

[25] D. Song, O. Macias, and S. Horiuchi, Phys. Rev. D **99**, 123020 (2019), 1901.07025.

[26] O. Macias, H. van Leijen, D. Song, S. Ando, S. Horiuchi, and R. M. Crocker, MNRAS (2021), 2102.05648.